



Control system design of reverse osmosis plants by using advanced optimization techniques

Adrian Gambier*, Andrea Wellenreuther, Essameddin Badreddin

*Automation Laboratory (PROAUT), Institute of Computer Engineering, Heidelberg University, 68131 Mannheim, Germany
Tel. +49 621 181-2783; Fax +49 621 181-2739; emails: {adrian.gambier, andrea.wellenreuther, badreddin}@ziti.uni-heidelberg.de*

Received 11 October 2008; Accepted in revised form 29 September 2009

ABSTRACT

A review about reverse osmosis (RO) desalination leads to the conclusion that the field of control system design of RO plants is still an open research subject. The standard approach considers two control loops with PI controllers. This is an economical viable solution for the control problem. However, the resulting control performance is normally suboptimal because controllers are individually tuned assuming inaccurately that the system is decoupled. In order to overcome this problem, some advanced control algorithms have been proposed in the specialized literature. However, such approaches are complicated and expensive. Therefore manufacturers of RO plants are not enthusiastic with their implementation particularly in the case of small plants. In the present work, an approach for the optimal achievement of controllers' parameters based in game theory and multi-objective optimization is applied to tune the PI controllers of a simple RO plant. The methodology allows a simultaneous tuning of several controllers distributed in different coupled control loops. Moreover, some control systems topologies are compared and an optimal solution for the control problem is proposed. Thus, the main objective here is to obtain the best possible performance for the control system without having to change control algorithms and equipment. Simulation results show the advantage of using the proposed approach and make apparent the control system topology, which yields the best tracking performance.

Keywords: PI control; Multi-loop control; Multi-objective optimization

1. Introduction

In the last years, significant advances in the membrane technology have allowed an essential improvement in the filtering quality and simultaneously a general reduction of costs such that RO plants have today lower energy consumption, investment cost, space requirements and maintenance than other desalination methods. Thus, RO plants require sensible components that should be preserved during a long operation in a high dependable manner. On the other hand, they should be maintained

working stable at its operating point under all possible working conditions. All these characteristics can be improved by means of an optimal control system design (see the overview presented in [1]).

The first multi-loop control system for RO plants is proposed in [2], where one pressure controller and two pH controllers are included and a simple control system topology is assumed. Afterward, control systems for reverse osmosis desalination plants have been studied in the literature by using PID as well as Model Predictive Control laws (MPC) in, for example, (but not only) [3–8].

In [8], an approach based on DMC (Dynamic Matrix Control) is compared with standard PID control. Here,

* Corresponding author.

the linear dynamic model proposed by [2] is utilized to design a multi-loop control system with two PI controllers, which are designed to work with coupled variables. A MPC approach is proposed and compared with PID control in [4]. Decoupled control is proposed in [7]. A preliminary study about optimal PI multi-loop control is presented in [6]. Non-linear MPC for a high recovery RO system is proposed in [9]. A controller based on fuzzy logic is proposed in [10]. Finally, a FDI/FTC simulation study on a RO model under actuator faults is the subject of [11] and a real-time implementation of a FTC based in switching control is studied [12].

The design using advanced control techniques normally requires a parametric dynamic model that has to capture the dynamic behavior but enough simple to be used in the design. A simplified model for an industrial plant is reported in [13]. Dynamic models for RO plants have first been reviewed in [14], and more recently in [15]. The conclusion is that this field still requires more research efforts. A nonlinear lumped-parameter model using first-principles and its parameters are computed from experimental data is derived in [5].

The implementation of advanced control systems has two disadvantages from the manufacturers' point of view: On one hand, more expensive control equipment is required and, on the other hand, a more specialized user is needed. Therefore, it is often desired a conventional but optimal tuned control system. This is the main objective of this work, which proposes the joint optimization of all control loops by using game theory and multi-objective optimization. In addition, several control system topologies are studied and compared.

2. The reverse osmosis plant and its control loops

A basic RO system normally consists of four main sub-systems: pretreatment, high-pressure pump, membrane assembly (RO unit) and post-treatment (Fig. 1). Salty feed water is first pretreated to avoid membrane fouling. It then passes through filter cartridges (a safety device) and is sent through the membrane modules (permeators) by a

high-pressure pump. Because of the high pressure, pure water permeates through the membranes and the salty water becomes very concentrated (brine). The water product flows directly from the permeators into a storage tank, and part of the brine (at high pressure) is sent via an energy recovery system back into the water source and the rest is discharged (see [16] for a review about different desalination processes).

Pretreatment is important in RO plants because the membranes' surfaces have to be permanent clean. Thus, suspended particles must be removed before they reach the membrane. Moreover, microbial growth on the membranes has to be avoided. Hence, the pretreatment consists of fine filtration and the addition of chemicals to inhibit precipitation and the growth of microorganisms. The high-pressure pump supplies the pressure needed to enable the water to pass through the membrane. This pressure range is from 15 to 25 bar for brackish water and from 54 to 80 bar for seawater.

The membrane assembly consists of a pressure vessel and several membrane units that permit the feed water to be pressurized against the membrane. The membrane must be able to resist the entire pressure drop across it. The post-treatment consists of stabilizing the water and preparing it for distribution. This post-treatment might consist for example of the removing gases such as hydrogen sulfide and adjusting the pH.

From the systemic point of view, a RO desalination plants has four variables of interest: (1) flow rate of permeate, (2) conductivity of permeate, (3) trans-membrane pressure, and (4) inlet pH value. The first two outputs are obviously important because they are production targets. Trans-membrane pressure must not be allowed to exceed an upper limit since that could cause membrane rupture. Moreover, this variable regulates the production outputs. The inlet pH value should be within bounds to extend membrane life. It also affects the conductivity of permeate. Two manipulated variables are available to control the system: (1) flow rate of retentate (acting on the transmembrane pressure) and (2) the flow rate of acid at the inlet (modifying the inlet pH value). An il-

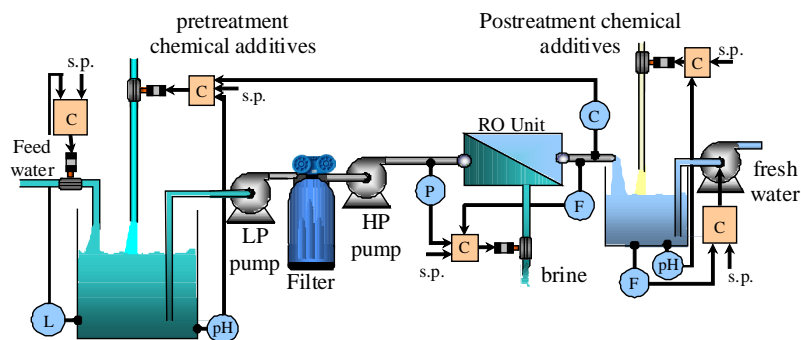


Fig. 1. Schematic diagram of a simple RO plants.

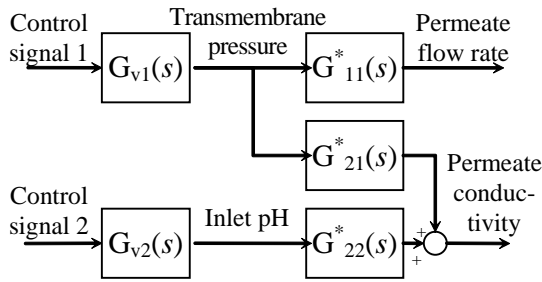


Fig. 2. Block diagram of a standard RO plant.

Illustrative block diagram is shown in Fig. 2. Notice that the system is coupled in one direction, i.e. changes in the transmembrane pressure affects the permeate conductivity but changes in the inlet pH value are not reflected in the membrane flow rate. Thus, the system is said to be inferior triangular.

The main objective of the control system of a RO plant is to maintain a constant production rate with acceptable purity. Moreover, control has also the function to protect some sensible components as for example the membranes. Hence, the control system consists of two main control loops: (1) permeate flow rate by changing the trans-membrane pressure with the control valve at the end of the brine pipeline, and (2) the permeate conductivity, which is controlled by manipulating the chemicals at the feed water inlet. These control loops can be complemented by using two cascade structures adding pressure to the first control loop and pH value of feed water to the second one. Moreover, several minor control loops can be found as for example, level control of pre-treatment and post-treatment tanks and pH control of permeate, as it is suggested in Fig. 1.

The mathematical model at the operating point ($u_{10} = 50\%$, $u_{20} = 50\%$, $F_0 = 0.25 \text{ m}^3/\text{h}$, $C_0 = 425 \text{ mS/cm}$) used for the control system design is given by the following transfer functions

$$G_{11}(s) = G_{11}^*(s)G_{v1}(s) = \frac{B_{11}(s)}{A_{11}(s)} = \frac{-5.71(s+0.05)}{s^3 + 34.00s^2 + 355.56s + 222.23} \quad (1)$$

$$G_{21}(s) = G_{21}^*(s)G_{v1}(s) = \frac{B_{21}(s)}{A_{21}(s)} = \frac{33.78(s+2.86)}{s^3 + 5.36s^2 + 6.42s + 2.19} \quad (2)$$

and

$$G_{22}(s) = G_{22}^*(s)G_{v2}(s) = \frac{B_{22}(s)}{A_{22}(s)} = \frac{24.44(s+3.31)}{s^3 + 3.91s^2 + 4.40s + 1.52} \quad (3)$$

Similar transfer functions can be found, for example, in [2,4,7,8].

3. Standard control system

The standard control system used for RO plants consists of two control loops with two PI or PID controllers as it shown in Fig. 3.

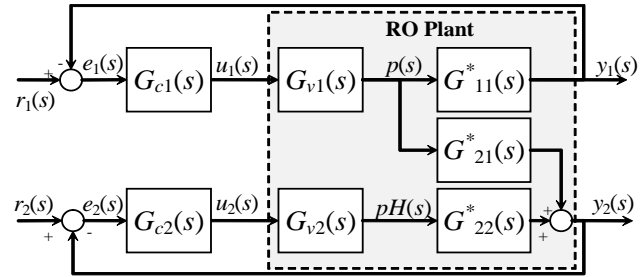


Fig. 3. Standard control loops for RO plants.

Normally, controllers' parameters are separately adjusted. The superior control loop is tuned first followed than by the lower one. Assuming that parameters can optimally found for both controllers, it is possible to obtain a behavior as shown in Fig. 6 (solid red curves).

Because of the interaction from the superior control loop to the inferior one, changes in the permeate flow rate affect the conductivity. One approach for handling this problem is known as decoupling [17]. However, decoupling is not always possible without performance degrading. In order to overcome this problem, a new approach has been proposed in [18] and it will be applied in this work to obtain the controllers' parameters.

4. Formulation of the game theoretic control system design

The theoretic description of the approach was already presented in [18] and it is summarized here for the sake of completeness. Controllers of an interacting multi-loop control system are viewed here as players of a nonzero-sum dynamic cooperative game. For such kind of games, cost functions (payoffs), one for each controller, are defined so that the performance criterion becomes a vector-valued function, i.e.

$$\mathbf{J} = [J_1 \quad J_2 \quad \dots \quad J_m]^T \quad (4)$$

where m is the number of players. Let $\mathbb{R}(s)^{m \times \ell}$ denote now the ring of $m \times \ell$ matrices whose elements are defined in $\mathbb{R}(s)$ a field of rational functions of the complex variable s with real coefficients. The dynamic game is now described by a linear time-invariant lumped closed-loop system given by

$$\mathbf{E}(s) = \{e_i(s) \in \mathbb{R}(s) \mid e_i(s) = r_i(s) - y_i(s), i = 1, \dots, m\} \quad (5)$$

where $r_i(s) \in \mathbf{R}(s) \subset \mathbb{R}(s)$ are reference functions and the output variable y_i is obtained from

$$\mathbf{Y}(s) = \{y_i(s) \mid y_i(s) = \sum_{j=1}^{\ell} G_{ij}(s)u_j(s), i = 1, \dots, m\} \quad (6)$$

$G_{ij}(s) = B_{ij}(s) / A_{ij}(s) \in \mathbb{R}(s)$ is assumed to be causal. Polynomials A_{ij} and B_{ij} are defined as

$$\begin{aligned} A_{ij}(s) &= s^{n_a} + a_{ij,1}s^{n_a-1} + \dots + a_{ij,n_a} \text{ and} \\ B_{ij}(s) &= b_0s^{n_b} + b_{ij,1}s^{n_b-1} + \dots + b_{ij,n_b} \end{aligned} \quad (7)$$

respectively. Variable $u_j(s) \in \mathbf{U}(s) \subset \mathbb{R}(s)$ is the control variable used by the player j to act upon the game. The dynamic game behavior is now described as

$$f : \mathbf{R}(s) \times \mathbf{U}(s) \times \mathbb{R}(s)^{m \times \ell} \rightarrow \mathbf{E}(s) \quad (8)$$

In compacted matrix notation, it is

$$\mathbf{e}(s) = \mathbf{r}(s) - \mathbf{G}(s)\mathbf{u}(s) \quad (9)$$

where $\mathbf{G}(s) \in \mathbb{R}(s)^{m \times \ell}$. A graphic description of this representation is given in Fig. 4.

Control variables u_j (for $j = 1, \dots, \ell$) are obtained by multi-objective optimization (MOO) of the objective vector \mathbf{J} , whose each element is defined by

$$J_i : \mathbf{E}(s) \times \mathbf{U}(s) \rightarrow \mathbb{R}^+ \cup \{0\}, \quad i = 1, \dots, m \quad (10)$$

Players are assumed now to be dynamically governed by the control law

$$u_i(s) = \frac{T_{ij}(s)}{P_{ij}(s)} r_j(s) - \frac{Q_{ij}(s)}{P_{ij}(s)} y_i(s) \quad (11)$$

where $T_{ij}(s)/P_{ij}(s)$ and $Q_{ij}(s) \in \mathbb{R}(s)$. Polynomial T , Q and P are then defined as

$$\begin{aligned} T_{ij}(s) &= s^{n_i} + t_{ij,1}s^{n_i-1} + \dots + t_{ij,n_i}, \\ P_{ij}(s) &= s^{n_p} + p_{ij,1}s^{n_p-1} + \dots + p_{ij,n_p} \text{ and} \\ Q_{ij}(s) &= q_{ij,0}s^{n_q} + q_{ij,1}s^{n_q-1} + \dots + p_{ij,n_q}. \end{aligned} \quad (12)$$

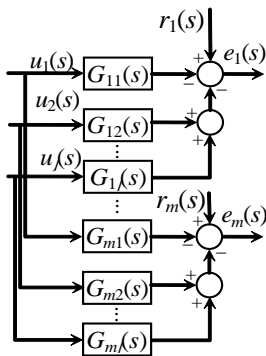


Fig. 4. Block diagram for the general structure of dynamic game.

Real coefficients of polynomials (12) can be summarized in a parameter vector $\theta_{c_{ij}} \in \mathbb{R}^{n_i+n_j+n_p+1}$

$$\theta_{c_{ij}} = [t_{ij,1} \dots t_{ij,n_i} \mid p_{ij,1} \dots p_{ij,n_p} \mid q_{ij,0} \dots q_{ij,n_q}]^T \quad (13)$$

In this case, the multi-objective optimization problem requires optimizing the objective functions

$$J_i : \mathbb{R}^{n_i+n_j+n_p+1} \rightarrow \mathbb{R}^+ \cup \{0\}, \quad i = 1, \dots, m \quad (14)$$

subject to the constraints given by Eqs. (9) and (11) in order to solve the game.

For this work, objective functions are defined as

$$J_i = \int_0^\infty L[e_i(t), u_{si}(t)] dt = \frac{1}{2\pi j} \int_{-j\infty}^{j\infty} L[e_i(s), u_{si}(s)] ds \quad (15)$$

for $i = 1, \dots, m$ where

$$L[e_i(s), u_{si}(s)] = e_i(s)e_i(-s) + \lambda_i u_{si}(s)u_{si}(-s) \quad (16)$$

$\lambda_i \in \mathbb{R}^+$ is a free design parameter. Furthermore, $u_{si}(s) = s u_i(s)$, where $u_i(s)$ is obtained from (11) and e_i is the i -th row of (9).

The simultaneous optimization of all cost functions is carried out by means of a multiobjective optimization (MOO) algorithm, which leads to a Pareto optimal set. The final solution is given by a decision maker, tacking one optimal solution from the Pareto front (see [19] for details).

The MOO optimization problem is solved by using MOGA (Multiple Objective Genetic Algorithm, [20,21]). It simulates the survival of the fittest in biological evolution by means of algorithms. The renewal of a population (entire set of variables that represent a group of potential solution points) is based on the so called *genetic operators*: recombination (out of two points of the population picked out so that a new point is generated, e.g. by averaging), mutation (single, randomly selected digits of a newly generated point are substituted by a realization of a random variable) and selection (out of the union of the original population and the newly generated points, which are taken over into the new population with the best fitness).

5. Additional considerations

The parametric optimization can lead to unacceptable results in case of model mismatch. In order to solve this inconvenient two approaches, which can directly be included in the optimization task, are available. The first one is given in [22]. It consists in selecting the final solution from the Pareto set according to the minimum *structured singular value* μ such that the obtained controller is the most robust contained within the Pareto set for a given uncertainty. The other one requires the uncertainty model given as interval polynomials. The multi-objective optimization process yields the controller's parameters as

the best compromise for all models within the given family (see [23] for details).

Finally, the control design approach proposed here does not include process disturbances in order to simplify the presentation. However, it is possible to introduce disturbances in the approach as it is already described in [24].

6. Game theoretic control system design for the RO plant

Following the design described in the previous section and using the model presented in Section 2, controllers for the RO plant are obtained in the current section. PI control laws are used such that Eq. (11) simplifies to

$$u_i(s) = \frac{Q_{ij}(s)}{P_{ij}(s)} [r_j(s) - y_j(s)] \quad (17)$$

where polynomial P and Q are given by

$$P_{ij}(s) = s \quad (18)$$

and

$$Q_{ij}(s) = K_{ij}s + K_{ij}/T_{ij} \quad (19)$$

where $i = 1, 2$ and $j = 1, 2$. The design is based on a step reference signal $r_i(s) = r_{oi}/s$. Variables $e_i(s)$ and $u_{si}(s)$ are obtained from the closed-loop system as

$$e_1(s) = \frac{A_{11}P_{11}r_1}{P_{11}A_{11} + Q_{11}B_{11}} = \frac{A_{11}P_{11}r_1}{A_{11}^*} \quad (20)$$

$$u_{s1}(s) = \frac{sA_{11}Q_{11}r_1}{A_{11}^*} \quad (21)$$

$$e_2(s) = \frac{A_{22}P_{22}(A_{21}A_{11}^*r_2 + B_{21}A_{11}Q_{11}r_1)}{A_{21}A_{11}^*A_{22}^*} \quad (22)$$

where $A_{22}^* = A_{22}P_{22} + B_{22}Q_{22}$ and

$$u_{s2}(s) = \frac{sA_{22}Q_{22}(A_{21}A_{11}^*r_2 + B_{21}A_{11}Q_{11}r_1)}{A_{21}A_{11}^*A_{22}^*} \quad (23)$$

The free design parameters λ_1 and λ_2 were set to 0.0001 and 2, respectively. Algorithms and parameters used for the MOGA are summarized in Table 1.

Table 1
Algorithms and parameters for the MOO

Evolutionary algorithm	Values
Number of generations and chromosomes	650, 4
Subpopulations	6
Individuals (at start per subpopulation)	50, 40, 40, 50, 60, 60
Number of objective functions	2
Algorithm for the selection	Stochastic universal sampling
pressure	2.1
gen. gap	0.9
Algorithm for the reinsertion	Local reinsertion
rate	1
Algorithm for the recombination	Discrete recombination
rate	1
Algorithm for the mutation	Real valued mutation
rate	1
range	0.1

The optimization process yields to the optimal Pareto set given in Fig. 5 and the corresponding parameters of the PI controllers are summarized in Table 2.

In order to analyze the obtained controllers, simulation studies were carried out for all controllers by using Matlab/Simulink. Controllers were implemented according to Eq. (17) including an anti-reset wind-up mechanism.

The plant was set at the operating point given by valve openings of 50%. In this case, the permeate flow rate is 0.25 m³/h and the permeate conductivity 425 μ S/cm. The experiment consists in changing the set point for the permeate flow rate first to 0.35 m³/h after 30 s and to 0.30 m³/h after 4 min. The permeate conductivity set point was changed only once from 425 to 440 μ S/cm after 2.5 min. Simulation results are shown in Fig. 6. Solid curves represent the control system tuned using standard methods and the dashed ones, the control system tuned by the new method.

The standard control system shows an excellent performance for the permeate flow rate control loop because it was specifically tuned for it without taking care the performance in the conductivity control loop. The new method provides a more equilibrated solution for both control loops.

Table 2
Parameters for the PI controllers

	Controller 1		Controller 2			Average cost	
	K_{11}	T_{11}	J_{11}	K_{22}	T_{22}		J_{22}
Standard control system	-0.7331	0.8122	0.0314	0.8835	2.9897	413.2	206.6
New control system	-0.6524	0.5834	0.1463	0.0643	1.6728	336.6	168.3

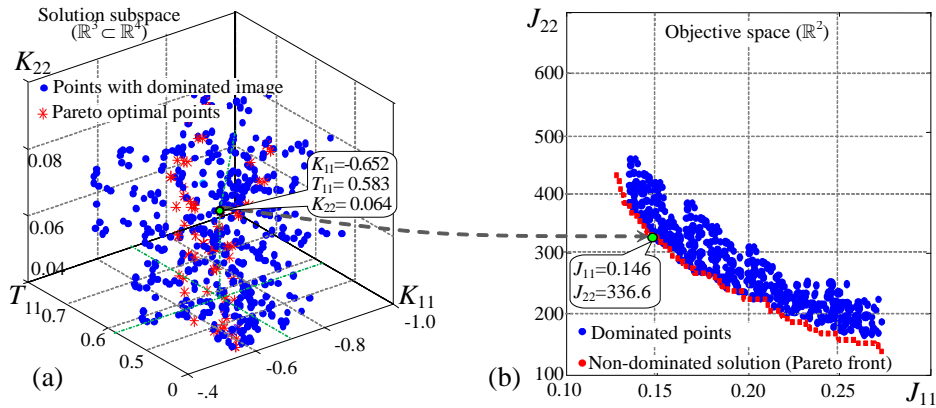


Fig. 5. Optimal Pareto set for the given example. (a) Solution space for three parameters (K_{11} , T_{11} , K_{22}), (b) Objective space (J_{11} , J_{22}) and the optimal Pareto set.

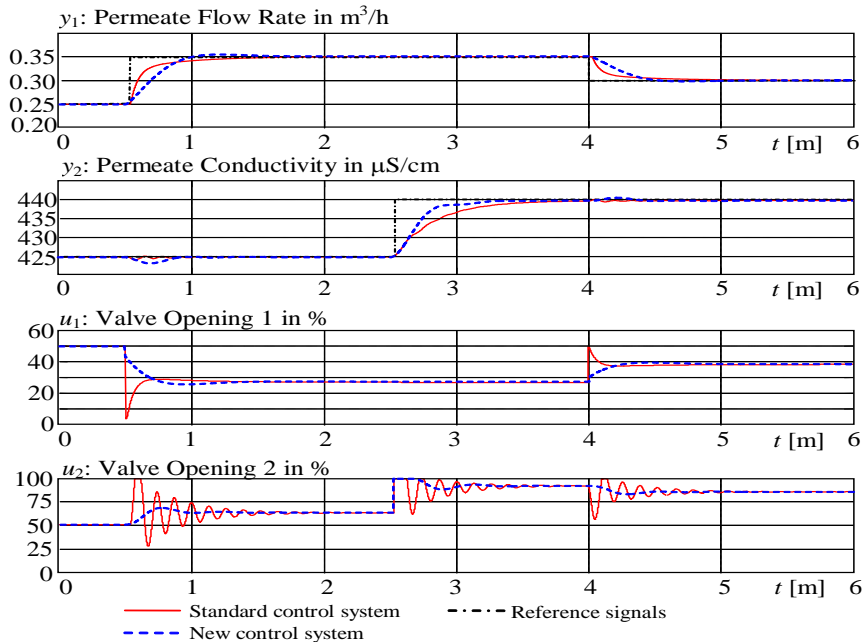


Fig. 6. Simulation results for the RO control systems.

Changes in the set point of the permeate flow rate introduces a disturbance in the second control loop. This disturbance cannot be adequately managed by the standard control system. Contrarily, the control system designed by using the new approach provided an excellent performance for the coupled system.

7. Other control system topologies

The plant described in Fig. 2 is an inferior triangular system, i.e. the interaction is present only in one direction (from the first input to the second output) through the transfer function G_{21} . Hence, changes in the first input are

reflected as disturbances in the second output. Contrarily, changes in the second input do not affect the first output.

The standard control system topology described in Fig. 3 maintains the inferior triangular shape of the plant. Its advantage is the decoupling from the second control loop to the first one. However, this control system has two disadvantages. On one hand, it is possible to observe from Eq. (22) that poles of G_{21} cannot be changed by these control topologies, so that this open-loop behavior is also present in the closed-loop system. On the other hand, the amplitude of disturbances in the second control loop due to the interaction can only be decreased by reducing the amplitude of the first control signal, which in turn makes

the first control loop slower. As a result, the best result is a compromise between acceptable level of disturbance in the second control loop and the reaction time of the first one.

The above described analysis leads to the question if it is possible to improve the performance of the control system by modifying the control system topology. It is clear that modifications that preserve the inferior triangular structure will have similar properties as the system of Fig. 3 with a possible better compromise. Alternatively, modifications that do not maintain the triangular structure will allow changing the poles of G_{21} but at the cost of introducing disturbances from the second control loop to the first one. In the following, some variants for the control system topology are studied (see [25] for a game theoretic analysis of these topologies).

7.1. Modifications that preserve the triangular structure

7.1.1. Additional controller from the first to the second control loop

The control system is modified as shown in Fig. 7. The additional controller can be used as a decoupler if the resulting transfer function is realizable or as a feed forward control for a pre-compensation of the effects of the control signal u_1 on the output y_2 .

The transfer function for the control error of the first control loop is the same as for the standard case [Eq. (20)]. The transfer function for the second control loop is now

$$e_2(s) = \frac{P_{22} [A_{21}A_{22}P_{21}A_{11}^*r_2 - A_{11}T_1^*r_1]}{A_{21}P_{21}A_{11}^*A_{22}^*} \quad (24)$$

where $T_1^* = B_{21}A_{22}Q_{11}P_{21} + B_{22}A_{21}Q_{21}P_{11}$ and the third controller is $G_{c3}(s) = Q_{21}(s)/P_{21}(s)$. Notice the presence of A_{21} in the denominator, i.e. roots of A_{21} cannot be modified by the introduction of this new controller.

7.1.2. Proportional controller from the first to the second control loop

A particular case of the control system presented in Fig. 7 is given in Fig. 8, where the third controller is defined by $G_{c3}(s) = K_{12} G_{c1}(s)$.

The transfer function for the first control loop is given by Eq. (20) and the transfer function of the second control loop is in this case

$$e_2(s) = \frac{P_{22} (A_{21}A_{22}A_{11}^*r_2 - A_{11}Q_{12}T_1^*r_1)}{A_{21}A_{11}^*A_{22}^*} \quad (25)$$

where $T_1^* = B_{21}A_{22} + B_{22}A_{21}K_{12}$.

The advantage of this control system is that there is one parameter less to be optimized and from the point of view of the implementation no additional controller is necessary.

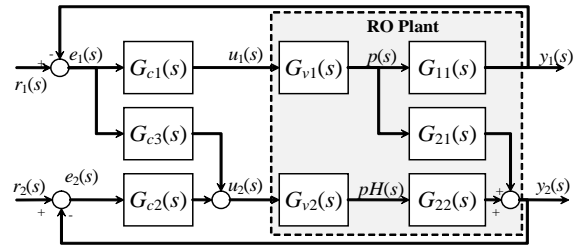


Fig. 7. Control system with an additional controller from the first to the second control loop.

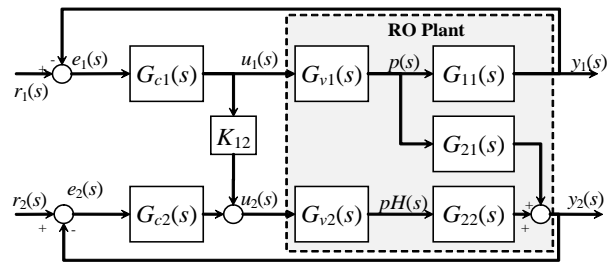


Fig. 8. Particular case of Fig. 7 for $G_{c3}(s) = K_{12} G_{c1}(s)$.

7.1.3. Cascade control for the second control loop

Another way to introduce the first output in the second control loop is by using a cascade structure. The resulting scheme is shown in Fig. 9.

The transfer function of the first control loop is, as for all previous cases, Eq. (20) and the transfer function for the second control loop becomes now

$$e_2(s) = \frac{P_{22} (A_{21}A_{22}P_{21}A_{11}^*r_2 - Q_{11}T_1^*r_1)}{A_{21}A_{11}^* (A_{22}P_{21}P_{22} + B_{22}Q_{21}Q_{22})} \quad (26)$$

where $T_1^* = B_{11}B_{22}A_{21}Q_{21} - B_{11}A_{11}A_{22}P_{21}$ and the third controller is $G_{c3}(s) = Q_{12}(s)/P_{12}(s)$.

7.2. Modifications that do not maintain the triangular structure

7.2.1. Additional controller from the second control loop to the first one

In a similar way as in the previous section, an additional controller can be introduced to the control system but now according to Fig. 10.

Notice that now both transfer functions changes, i.e.

$$e_1(s) = \frac{P_{11} (A_{11}T_1^*r_1 - B_{11}A_{21}A_{22}Q_{12}P_{22}r_2)}{A_{21}P_{12}A_{11}^*A_{22}^* + B_{21}A_{11}A_{22}Q_{12}P_{11}P_{22}} \quad (27)$$

where $T_1^* = A_{21}^*A_{22}P_{22} + B_{22}A_{21}Q_{22}P_{12}$ with $A_{21}^* = A_{21}P_{12} + B_{21}Q_{12}$ and

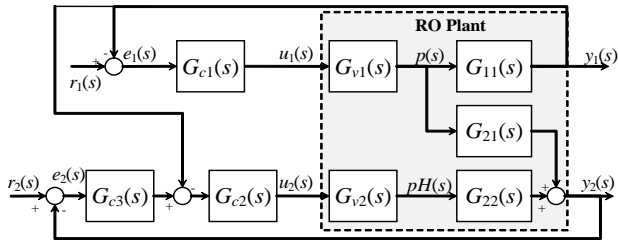


Fig. 9. Cascade control on the second control loop.

$$e_2(s) = \frac{A_{22}P_{12}P_{22}(A_{21}A_{11}^*r_2 - B_{21}A_{11}Q_{11}r_1)}{A_{21}P_{12}A_{11}^*A_{22}^* + B_{21}A_{11}A_{22}Q_{12}P_{11}P_{22}} \quad (28)$$

It is important to remark here that no pole of the open loop system holds in the closed loop system. The cost to pay is that transfer functions are considerably more complicated.

7.2.2. Proportional controller from the first to the second control loop

A particular case of the control system presented in Fig. 10 is given in Fig. 11, where the third controller is given by $G_{c3}(s) = K_{12} G_{c1}(s)$. Transfer functions become in this case

$$e_1(s) = \frac{A_{11}P_{11}T_1^*r_1 - B_{11}A_{21}A_{22}Q_{22}P_{11}K_{12}r_2}{A_{21}A_{11}^*A_{22}^* + B_{21}A_{11}A_{22}Q_{22}P_{11}K_{12}} \quad (29)$$

where $T_1^* = A_{21}A_{11}^* + B_{21}A_{22}Q_{22}K_{12}$ and

$$e_2(s) = \frac{A_{22}P_{22}(A_{21}A_{11}^*r_2 - B_{21}A_{11}Q_{11}r_1)}{A_{21}A_{11}^*A_{22}^* + B_{21}A_{11}A_{22}Q_{22}P_{11}K_{12}} \quad (30)$$

7.2.3. Cascade control system from the first control loop

Similarly to Case 7.1.3, a cascade control scheme can also be implemented in the first control loop. The obtained topology is shown in Fig. 12. Transfer functions for this case are

$$e_1(s) = \frac{P_{11}(A_{21}T_1^*r_1 + B_{11}B_{22}A_{21}Q_{12}Q_{22}r_2)}{A_{21}T_{12}^*A_{22}^* + B_{21}A_{21}A_{22}Q_{12}P_{11}P_{22}} \quad (31)$$

with $T_1^* = A_{11}P_{12}A_{22}^* + B_{21}Q_{12}P_{22}$, $T_{12}^* = A_{11}P_{11}P_{12} + B_{11}Q_{11}Q_{12}$ and

$$e_2(s) = \frac{A_{22}P_{22}(T_2^*r_2 - B_{21}A_{11}Q_{11}Q_{12}r_1)}{A_{21}T_{12}^*A_{22}^* + B_{21}A_{21}A_{22}Q_{12}P_{11}P_{22}} \quad (32)$$

where $T_2^* = A_{11}P_{11}A_{21}^* + B_{11}A_{21}Q_{11}Q_{12}$.

7.2.4. Double cascade control system

A two-cascade control system topology is indirectly

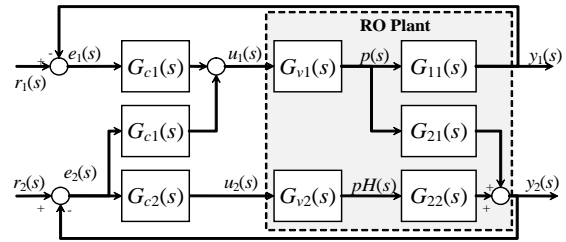


Fig. 10. Control system with cross-controller from the second control loop to the first one.

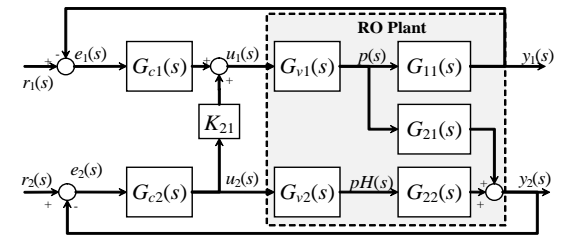


Fig. 11. Particular case of Fig. 10 for $G_{c3}(s) = K_{21} G_{c2}(s)$.

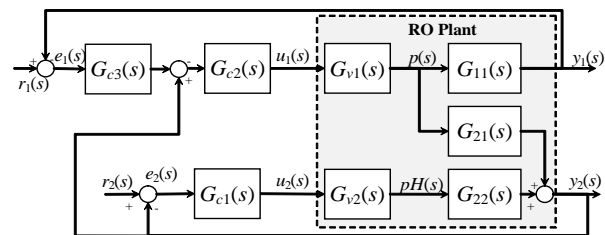


Fig. 12. Cascade control on the first control loop.

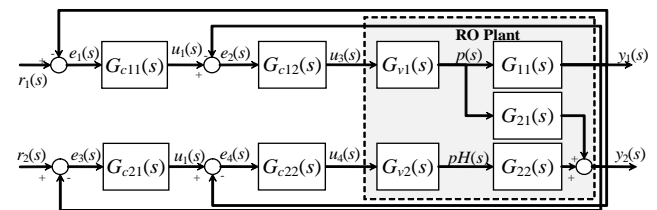


Fig. 13. Two-cascade control system.

suggested in [4] and implemented for digital controllers in [26]. The scheme combines the previous Cases 7.1.3 and 7.2.2 and it is shown in Fig. 13. A two-cascade control system is very complicated and requires a special study. Therefore, this case mentioned but not included in the present analysis.

7.3. Control system design and simulation results

Optimal controllers for all presented topologies can also be obtained by using the methodology proposed in

Section 4. Table 3 summarizes controllers' parameters and minimum values for the performance indices as well as an average cost value to evaluate a final decision.

Simulation results show that control topologies, which do not maintain the triangular structures, do not improve the control system performance of the inferior control structure even if all poles of open loop system can be changed.

An additional result is the fact that a third controller has a similar behaviour as a control system with a proportional cross factor from the first control loop to the second one (Case 7.1.2). Thus, the last mentioned control topology is so far the best obtained for this kind of plant.

Notice that this topology also brings the minimum value for the average cost.

8. Conclusions

In the present work, an approach oriented to improve the control performance maintaining the control algorithms, as well as the hardware and the software is presented. Moreover, control systems topologies for a simple reverse osmosis plant are evaluated and compared. The controller design is carried out by using joint optimization of all controllers. Here, controllers are assumed to use PI control laws. However, other control laws like PID

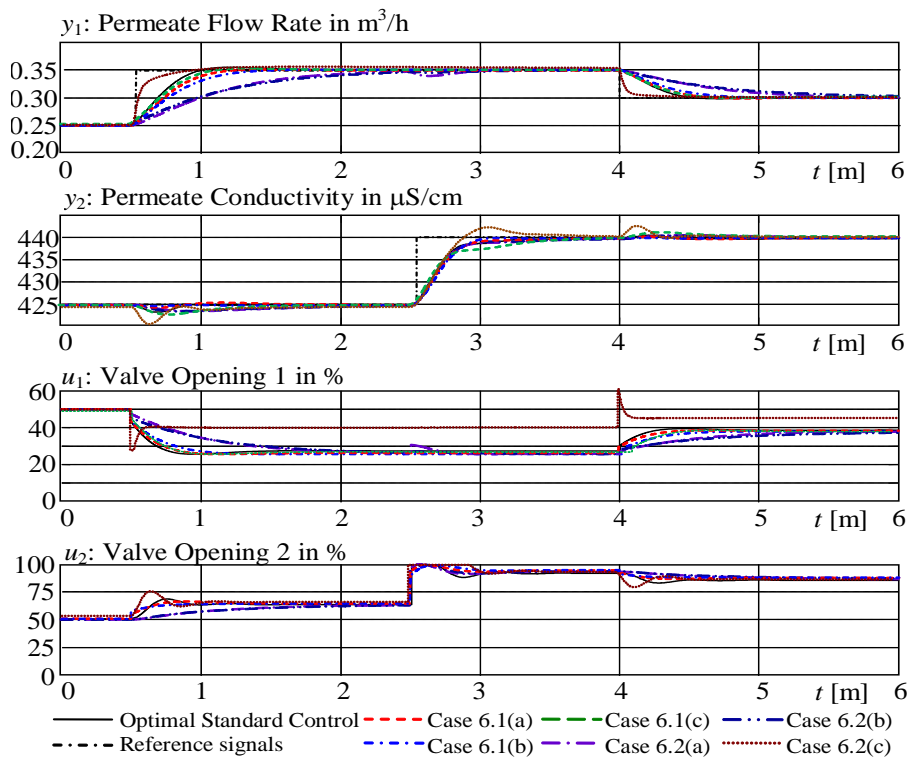


Fig. 14. Simulation results for the control systems of Section 7.

Table 3
Parameters for the PI controllers for the topologies of Section 7

Topology	Controller 11			Controller 22			Controller 12 or 21			Average cost
	K_{11}	T_{11}	J_{11}	K_{22}	T_{22}	J_{22}	$K_{12/21}$	$T_{12/21}$	$J_{12/21}$	
Case 7.1.1	-0.6527	0.9661	0.50	0.0231	3.9932	351.8	0.8499	2.1336	182.3	178.2
Case 7.1.2	-0.6007	0.6796	0.50	0.0186	2.2781	331.7	0.6599	—	—	166.1
Case 7.1.3	-0.1068	0.5379	0.47	2.9596	518.57	474.9	0.0127	3.3606	165.1	213.5
Case 7.2.1	-0.2306	0.6468	0.44	0.0241	2.4796	328.4	0.0025	59.815	326.1	218.2
Case 7.2.2	-0.4138	1.2654	0.40	0.0201	2.3680	359.5	-0.0214	—	—	179.9
Case 7.2.3	-22.8047	41.0248	2.603	0.0539	3.4900	339.2	0.4165	2.4269	193.7	178.5

controllers can also be optimized by the same method. Simulation results show that the control system obtained with this method is superior to PI controllers, which are tuned individually.

An additional observation is that sometimes simple multi-loop joint-optimised control systems seems to perform equivalently or still better than more sophisticated and difficult to implement control algorithms. However, this requires a more deeply study taking into consideration advanced control algorithms like for example constrained MPC, adaptive control and fault-tolerant control for linear as well as nonlinear systems. This is an excellent motivation for future work in the field.

Acknowledgment

This work has been supported by the European Commission by means of the project Open-Gain under contract No. 032535.

References

- [1] I. Alatiqi, H. Ettouney and H. El-Dessouky, Process control in water desalination industry: an overview, *Desalination*, 126 (1999) 15–32.
- [2] I. Alatiqi, A. Ghabris and S. Ebrahim, Measurement and control in reverse osmosis desalination, *Desalination*, 75 (1989) 119–140.
- [3] A. Abbas, Model-predictive control of a reverse osmosis desalination unit, *Desalination*, 194 (2006) 268–280.
- [4] J.Z. Assef, J.C. Watters, P.B. Desphande and I.M. Alatiqi, Advanced control of a reverse osmosis desalination unit. Proc. International Desalination Association (IDA) World Congress, Abu Dhabi, 1995, 5 (1995) 174–188.
- [5] A. Bartman, C. McFall, P.D. Christofides and Y. Cohen, Model predictive control of feed flow reversal in a reverse osmosis desalination process. *J. Proc. Contr.*, 19 (2009) 433–442.
- [6] A. Gambier, A. Wellenreuther and E. Badreddin, Optimal control of a reverse osmosis desalination plant using multi-objective optimization. Proc. 2006 IEEE Conference on Control Applications, Munich, October 4–6, 2006, pp. 1368–1373.
- [7] C. Riverol and V. Pilipovik, Mathematical modeling of perfect decoupled control system and its application: A reverse osmosis desalination industrial-scale unit. *J. Automated Methods Manage. Chem.*, 2005 (2005) 50–54.
- [8] M.W. Robertson, J.C. Watters, P.B. Desphande, J.Z. Assef and I.M. Alatiqi, Model based control for reverse osmosis desalination processes, *Desalination*, 104 (1996) 59–68.
- [9] C. McFall, A. Bartman, P.D. Christofides and Y. Cohen, Control of reverse osmosis desalination at high recovery. Proc. 2008 American Control Conference, Seattle, June 11–13, 2008, pp. 2241–2247.
- [10] M. Jafar and A. Zilouchian, Real-time implementation of a fuzzy logic controller for a seawater RO plant. Proc. 5th World Automation Congress, 13 (2002) 31–36.
- [11] C. McFall, P.D. Christofides, Y. Cohen and J.F. Davis, Fault-tolerant control of a reverse osmosis desalination process. Proc. 8th IFAC Symp. on Dynamics and Control of Process Systems, Cancun, June 6–8, 2007, 3 (2007) 163–168.
- [12] A. Gambier, N. Blümlein and E. Badreddin, Real-time fault-tolerant control of a reverse osmosis desalination plant based on a hybrid system approach. Proc. 2009 American Control Conference, Saint Louis, June 10–12, 2009, pp. 1598–1603.
- [13] N.M. Al-Bastaki and A. Abbas, Modeling an industrial reverse osmosis unit. *Desalination*, 126 (1999) 33–39.
- [14] M. Soltanieh and W.N. Gill, Review of reverse osmosis membranes and transport models. *Chem. Eng. Comm.*, 12 (1981) 279–363
- [15] A. Gambier, A. Krasnik and E. Badreddin, Dynamic modelling of a simple reverse osmosis desalination plant for advanced control purposes. Proc. 2007 American Control Conference, New York, July 11–13, 2007, pp. 4854–4859.
- [16] O.K. Buros, The ABCs of Desalting, International Desalination Association, Topsfield, Massachusetts, USA, 2000.
- [17] D.E. Seborg, T.F. Edgar and D.A. Mellichamp, *Process Dynamics and Control*. John Wiley & Sons, New York, 2004.
- [18] A. Gambier, A. Wellenreuther and E. Badreddin, A new approach to design multi-loop control systems with multiple controllers. Proc. 45th IEEE Conference on Decision and Control, San Diego, December 13–15, 2006.
- [19] A. Gambier, Digital PID controller design based on parametric optimization, Proc. 2008 IEEE Conference on Control Applications, San Antonio, September 3–5, 2008.
- [20] C.M. Fonseca, Multiobjective genetic algorithms with application to control engineering problems. Ph.D. thesis, University of Sheffield, Sheffield, UK, 1995.
- [21] C.M. Fonseca and P.J. Fleming, Multiobjective optimization and multiple constraint handling with evolutionary algorithms – Part I: A unified formulation. *IEEE Trans. Systems, Man, & Cybernetics, Part A: Systems & Humans*, 28 (1998) 26–37.
- [22] A. Wellenreuther, A. Gambier and E. Badreddin, Optimal multi-loop control design of a reverse osmosis desalination plant with robust performance. 17th IFAC World Congress, Seoul, July 6–11, 2008, pp. 10034–10039.
- [23] A. Gambier, Optimal PID controller design using multiobjective Normal Boundary Intersection technique. Proc. Asian Control Conference 2009, Hong Kong, August 27–29, 2009, pp. 1369–1374.
- [24] A. Wellenreuther, A. Gambier and E. Badreddin, Controller tuning of stochastic disturbed multi-loop control systems. Proc. 2008 IEEE Multi-conference on Systems and Control, San Antonio, 3–5 September 2008, pp. 287–292.
- [25] A. Wellenreuther, A. Gambier and E. Badreddin, Game theoretical analysis for choosing the topology in multi-loop control systems. Proc. 2008 American Control Conference, Seattle, June 11–13, 2008, pp. 3671–3676.
- [26] A. Gambier, A. Wellenreuther and E. Badreddin, Multi-loop control system design: A game theoretical approach for computer-controlled systems. Proc. 46th IEEE Conference on Decision and Control, New Orleans, December 12–14, 2007, pp. 1814–1819.